7th Australasian Hydraulics and
Fluid Mechanics Conference,
Brisbane, 18-22 August, 1980

The Fine-Scale Structure of the Velocity Field of Turbulent Jets

B.R. SATYAPRAKASH
Post Graduate Student, Department of Mechanical Engineering, The University of Newcastle
and
R.A. ANTONIA
Professor of Mechanical Engineering, The University of Newcastle

SUMMARY Moments, up to order eight and spectral densities of the velocity derivatives have been measured on the centreline of turbulent plane and circular jets. Some of the difficulties encountered in carrying out the measurements are discussed. A study of the effect of the low-pass filter cut-off frequency on the statistics of the derivative indicates that an appropriate value for this cut-off is about 1.75 f_η (f_η is the Kolmogorov frequency) and not f_η as used by a number of previous investigators. The value of the constant μ that appears in one of the hypotheses of Kolmogorov and Obukhov depends on the method used to determine it but a decrease in μ with increasing order of the moment is qualitatively established by two different methods. The spectral data are consistent with an increase at high frequencies of the spectral density with an increase in the turbulence Reynolds number.

1 INTRODUCTION

Champagne (1978) recently obtained new data on the fine structure of the velocity u in both atmospheric turbulent boundary layer and various laboratory flows with a view to examining the data for evidence of universal behaviour and local isotropy. Kolmogorov normalised spectral shapes were found to be universal in the sense that they described the high frequency spectral behaviour of all turbulent flow fields with a similar value of the turbulence Reynolds number. R_λ ($\equiv u'\lambda/\nu$, prime denotes rms value, λ is the Taylor microscale). The variation with R_λ of the spectral density was consistent with the reformulation by Kolmogorov (1962) and Obukhov (1962) of Kolmogorov's original similarity theory.

In this paper we present statistics of the derivative $\partial u/\partial t$ measured in both plane and circular jets with an aim to verify the spectral variation observed by Champagne and also to provide a further check of some of the assumptions made in the reformulation by Kolmogorov and Obukhov.

2 EXPERIMENTAL ARRANGEMENT AND TECHNIQUE

A detailed description of the plane jet facility may be found in Hussain & Clark (1977). Data were taken at an exit velocity U_j of 9.64 m/s corresponding to a Reynolds number $R_j = 2.04 \times 10^4$ (d = 3.18 cm). Circular jets of two different diameters (d = 2.54, 18 cm) were used. The 2.54 cm nozzle had a Batchelor-Shaw profile and was used with the jet facility described in Hussain & Zedan (1978). The 18 cm jet facility has been described by Husain & Hussain (1979), except that a new 18 cm dia. fibreglass nozzle was used for the present study. The exit Reynolds number R_j was 5.56×10^4 and 4.71×10^5 for d = 2.54, 18 cm respectively. Both plane and circular jet facilities are located in a large laboratory (University of Houston) with controlled temperature and humidity.

The velocity fluctuation was measured with a 2.5 μm dia. Wollaston (Pt-10% Rh) hot wire (length approx. 0.52 mm) operated by a DISA55M10 constant temperature anemometer at an overheat of 0.8. The frequency response of the wire and anemometer, determined by the square wave technique was estimated to extend to about 100 kHz for the present experimental conditions. The output signal from the anemometer was first passed through a DISA55D26 signal conditioner (dc - 100 kHz) primarily to subtract the dc component of the signal. The signal was subsequently passed through a Krohn-Hite model 3341 low-pass filter (f_{c1}) (48 dB/octave roll off) before analogue differentiation using an operational amplifier. No perceptible departure from linearity could be discerned up to 100 kHz in the response of the differentiator. The differentiator was designed for a gain of unity at 7 kHz. The output voltage from the differentiator was passed through another Krohn-Hite 3341 low-pass filter (f_{c2}, of identical frequency and phase characteristics to the pre-differentiation filter). Output signals from the two filters were fed to a DISA55D35 true rms meter to obtain the rms values of u and $\partial u/\partial t$. These signals were also recorded on a Hewlett-Packard 3960 FM-4 track tape recorder for subsequent processing of the data by a digital computer. Particular attention was given to the following:

(i) The averaging time (typically 180 s) used in the digital processing of the data was sufficient to ensure satisfactory convergence of moments up to order eight, of $\partial u/\partial t$.

(ii) The dynamic range of the signal processing equipment was sufficient to achieve closure of the tails of probability density functions of $(\partial u/\partial t)$.

(iii) The cut-off frequency settings f_{c1} and f_{c2} for the two Krohn-Hite filters were determined at each measurement location. f_{c1} was first set arbitrarily to a relatively high frequency, typically twice the upper limit of the spectral content of $\dot{u} \equiv \partial u/\partial t$. The spectral density $\phi_{\dot{u}}$ obtained using a real-time spectrum analyser (SD35), was displayed on the built-in oscilloscope of the analyser to determine f_{c1} visually. The frequency f_{min} of the lowest point on the spectrum, which occurs before the increase due to noise, can be easily determined. Since there is some noise contribution to the spectrum for $f < f_{min}$, the correct setting for the filter cut-off should be less than f_{min}. From the spectral display the frequency f_C ($< f_{min}$) at which $\phi_{\dot{u}}$ exceeds by 2dB that at f_{min} was accurately determined using the scope cursor. Both f_{c1} and f_{c2} were then set at this value. Although the choice of 2dB is somewhat arbitrary it was found that, at most measurement locations, the value of f_{c1} (or f_{c2}) was approximately $2f_\eta$ ($f_\eta \equiv U/2\pi\eta$, where U is the local mean velocity and η is the Kolmogorov length scale

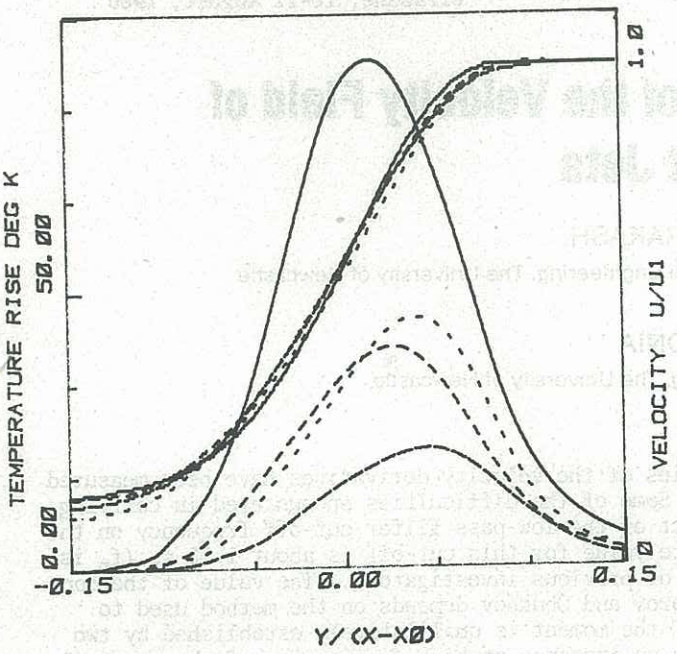

FIG. 4 Velocity and corresponding temperature profiles in reacting argon/argon shear layers.

evident in figures 1 and 2. Figure 3(b) is the simultaneous picture of ozone showing efficient penetration across the layer.

4 RESULTS

Figure 4 gives typical average temperature rise and velocity profiles in reacting shear layers in argon at 5 and 25 ms^{-1}. These and other results indicate that the effect of reactant concentration ratio on the skew of the temperature profile or the lateral position of its maximum is very small. Most notable, and in support of the flow pictures, is the fact that the velocity profile thickness appears unchanged by the heat release.

A question of considerable importance was to find out what oxidant concentration was required to burn practically all the fuel, i.e. to find the concentration of oxident where significant oxidant increase would produce negligible product increase. A series of runs were made with a nitric oxide concentration of 0.5%, increasing the ozone concentration from zero up to 7%, and measuring the maximum mean temperature rise. Figure 5 shows that above a concentration of about 5:1 very little further reaction product is obtained.

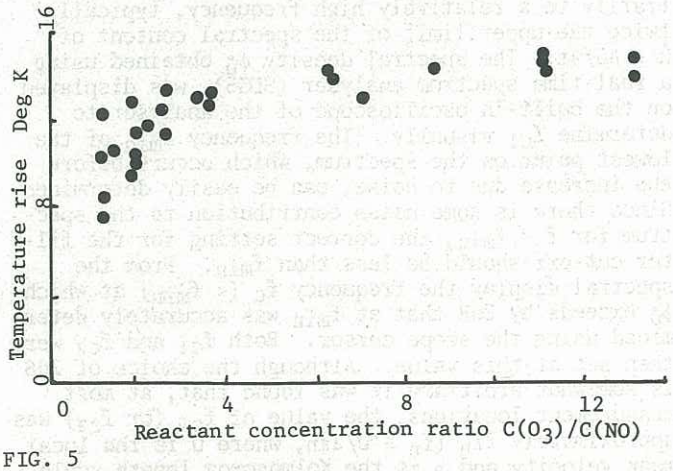

FIG. 5

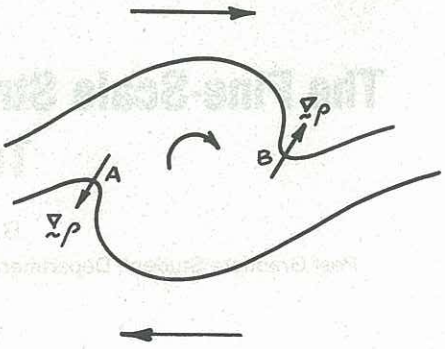

FIG. 6. Schematic large scale vortex structure.

5 CONCLUSIONS

It is clear that the entrainment flux of free stream fluid into the turbulent region is decreased with increasing heat release by an amount very closely compensating for the volume expansion within the layer. These results, and others not published here, indicate that the characteristic dominant large scales are still evident at temperature rises of 300°C, while small scales in the flow are progressively obliterated. These effects are consistent with the temperature dependence of viscosity. It is believed that the reduction in entrainment is a consequence of the baroclinic torque action. It can be shown that

$$\frac{Dw}{Dt} = -\frac{1}{\rho}\nabla\rho \times \frac{Du}{Dt}$$

If a "hot" structure similar to that in figures 1 and 2 is considered schematically, (figure 6), it can be seen that the only significant contribution to the vorticity field due to baroclinic torque is at points A and B in the same sense as the overall vorticity. Since the overall vorticity must remain constant, the effect is to inhibit the massive clumping of vorticity as evidenced in figure 1, thereby reducing the induced velocity field producing the entrainment.

6 ACKNOWLEDGEMENTS

Much of this work was undertaken as part of a Ph.D. candidature at the University of Adelaide in collaboration with Professor Garry Brown. Subsequent support is from CALTECH Subcontract F4960-79-C-0159.

7 REFERENCES

Toor, H.L. (1962), A.I.Ch.E., J8, 70.

Roshko, A. (1976), AIAA 76-78.

$\nu^{3/4}\,\bar{\varepsilon}^{-1/4}$, $\bar{\varepsilon}$ is the averaged rate of dissipation = $15\,\nu\,\overline{(\partial u/\partial x)^2}$, assuming local isotropy). For the present experimental conditions, $\phi_{\dot{u}}$ (f_{c1}) was typically 30dB below the maximum value of $\phi_{\dot{u}}$ which occurs at approximately $f_\eta/10$.

(iv) The spatial resolution of the sensor is clearly important in the study of the fine structure. The dia. d_w (2.5 μm) and length ℓ_w (≃ 0.52 mm) of the hot wire were chosen so that the ratio ℓ_w/η was as small as practicable. For x/D > 60, ℓ_w/η decreased from about 2.5 to 1.0. For sufficiently large ℓ_w/d_w, hot wire length corrections to the high frequency end of ϕ_u arise because the instantaneous wave number vector is not normal to the wire and because of inherent attenuation at extremely large wave numbers. Both effects worsen with increasing ℓ_w/η (Wyngaard, 1968). Wyngaard's calculations show that for a wire of length 3η, ϕ_u is underestimated by about 6% at $k_1\ell_w = 1$ ($k_1 = 2\pi f/U$; f is the frequency). For the present range of ℓ_w/η, no length corrections were made as these would fall within the scatter of the $\phi_{\dot{u}}$ data. It should be further noted that Wyngaard's calculations are based on a theoretical form of the spectrum which precludes any dependence on R_λ, at variance with the experimental observation of Champagne (1978). Once the experimental variation, at relatively large $k_1\eta$, of $\phi_{\dot{u}}$ with R_λ is established, Wyngaard's correction procedure could perhaps be modified so that the hot wire length correction also depends on R_λ.

3 RESULTS

The effect of varying the low-pass filter cut-off f_c (prior to digitizing) on the flatness factor F ($\equiv \overline{\dot{u}^4}/\overline{\dot{u}^2}^2$) for the plane jet is shown in Fig. 1. It is clear that F first increases with f_c before a maximum (or small plateau) is reached. With increasing f_c, the effect of the noise becomes more pronounced and F begins to decrease. A qualitatively similar behaviour of F vs f_c was observed by Kuo & Corrsin (1971) but the frequency at which the plateau was first reached was approximately equal to f_η. The data of Fig. 1 (and all the other data we have collected for both circular jets) indicate that a more appropriate value for this frequency is about 1.75 f_η. This particular setting for f_c, which is apparently independent of R_λ for the relatively small R_λ range considered here, has therefore been used for all present results. This value of f_c is in good agreement with the value (≃ $2f_\eta$) used by Gagne & Hopfinger (1979) but appreciably larger than the setting ($f_c = f_\eta$) of Frenkiel & Klebanoff (1975) who adopted the recommendation of Kuo & Corrsin. Frenkiel et al (1979) have verified that f_η is the appropriate setting at relatively low R_λ grid turbulence. Fig. 1 shows that the use of $f_c = f_\eta$ would on average underestimate F by about 12% in comparison to $f_c = 1.75\,f_\eta$. This error increases with order n, being equal to about 40% for n = 8.

To establish that the record duration chosen was sufficient to ensure stability of $\overline{\dot{u}^n}/\overline{\dot{u}^2}^{n/2}$ (at least for small values of n) two different methods were tried. First the expression derived by Tennekes & Lumley (1972, p.212) indicated that for the present record duration the mean square relative error for $\overline{\dot{u}^8}$ and of integral time scales of ($\dot{u}^4$ - $\overline{\dot{u}^4}$). The time required for convergence of the running moment of $\dot{u}^4$ to within 5% of its final value was also determined. This value is significantly smaller than the record duration.

The Reynolds number dependence of higher even order

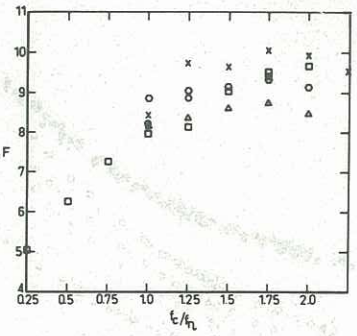

Figure 1 Variation of F with cut-off f_c for plane jet. ○, x/d = 80; □, 100; ⬡, 120; △, 140; x, 160

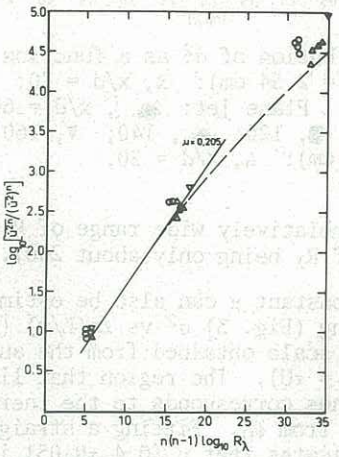

Figure 2 Reynolds number dependence of $\overline{\dot{u}^{2n}}/\overline{\dot{u}^2}^n$ (n = 2, 3, 4). Circular jet: ○, d = 2.54 cm; ▽, 18 cm; Plane jet: △; ---, Frenkiel & Klebanoff (1975)

moments $\overline{\dot{u}^n}/\overline{\dot{u}^2}^{n/2}$ (for n = 4, 6, 8) is plotted in Fig. 2 using a method suggested by Frenkiel & Klebanoff (1975). This method is based on the expression, hypothesised by Kolmogorov and Obukhov, for the variance σ^2 of the logarithm of the locally averaged dissipation

$$\sigma^2 = A + \mu\,\ell n(L/r) \qquad (\eta \ll r \ll L) \qquad (1)$$

where A depends on the nature of the large structure of length scale L, r is a characteristic dimension of the averaging volume (here $\dot{u}^2$ was averaged over a time interval τ, interpreted as r/U using Taylor's hypothesis) and μ is assumed to be a universal constant. For very large R_λ, A was neglected and, assuming lognormality of locally averaged $\dot{u}^2$, Frenkiel & Klebanoff found that

$$\overline{\dot{u}^{2n}}/\overline{\dot{u}^2}^n \sim R_\lambda^{3/4\,\mu n(n-1)} \qquad (2)$$

the explicit Reynolds number dependence arising by setting $r = \eta$ and using the result $L/\eta \propto R_\lambda^{3/2}$ for isotropic turbulence (e.g. Tennekes & Lumley, 1972). The present data lie slightly above the distribution of Frenkiel & Klebanoff, as a result of the setting of f_c. For $f_c = f_\eta$, the agreement (see Antonia & Danh, 1977) with Frenkiel & Klebanoff's distribution is quite satisfactory. Frenkiel & Klebanoff concluded that the decrease of μ (the local slope in Fig. 2) with n (note that the method of plotting emphasises n while reducing the importance of R_λ) is not necessarily due to an insufficiently large R_λ, since available atmospheric data for $\overline{\dot{u}^{2n}}$, at least for relatively small n, also fell on the same distribution. Frenkiel et al (1979) provided further support for this conclusion by showing that for the same flow (grid turbulence) the same distribution

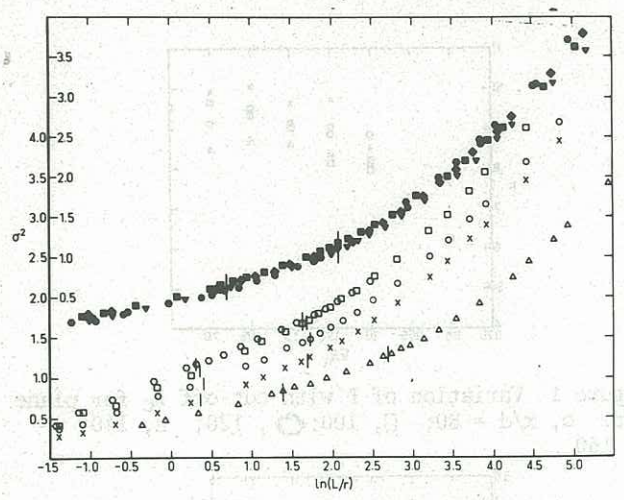

Figure 3 Distribution of σ^2 as a function of r. Circular jet (d = 2.54 cm): x, x/d = 70; ⊙, 80; ⊡, 90; ◇, 120. Plane jet: ⬬, x/d = 60; ●, 80; ▲, 100; ■, 120; ◆, 140; ▼, 160. Circular jet (d = 18 cm): Δ, x/d = 50.

applied over a relatively wide range of R_λ (the maximum value of R_λ being only about 200).

The universal constant μ can also be estimated by directly plotting (Fig. 3) σ^2 vs $\ell n(L/r)$ (L is the integral length scale obtained from the autocorrelation of u and $r = \tau U$). The region that lies between the vertical lines corresponds to the inertial subrange estimated from $\phi_{\mathring{u}}$. Fitting a straight line to this region indicates that μ (0.4 ±0.03) is twice as large as the slope inferred from the plot of Fig. 2. The other rather interesting result of Fig. 3 is the constancy of A in the plane jet. In the circular jet (d = 2.54 cm), A first increases with x/d but appears to reach a constant value at x/d ≃ 120. It should be emphasised that for both plane and circular jets the ratio of L to the half-width (or half-radius) was constant for the present range of x/d while mean and rms velocity profiles at different sections of the jets, and the variation of higher order moments of $\mathring{u}$ along the centreline were consistent with self-preserving development of the flows. It is not clear how sensitive A is as an indicator of the macrostructure of the flow. The *prima facie* inference that can be drawn from Fig. 3 is that the macrostructure is more quickly established in the plane than in the circular jet. This seems a little surprising since it is expected (e.g. Gutmark & Wygnanski, 1976) that the far field flow of the

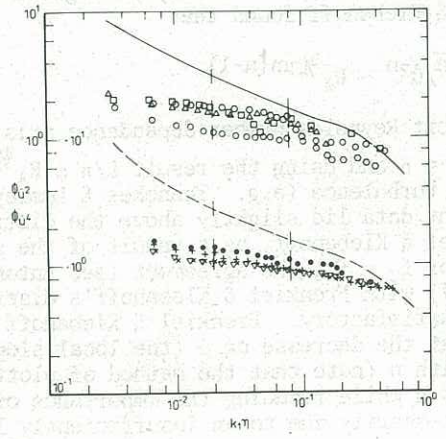

Figure 4 Spectra of $\mathring{u}^2$ and $\mathring{u}^4$. Plane jet ($\mathring{u}^4$): □, x/d = 80; o, 100; Δ, 120; ◇, 160; ——, $\mathring{u}^2$. Circular jet (d = 2.54 cm, $\mathring{u}^4$): x, x/d = 70; ▽, 80; ●, 90; +, 120; ----, $\mathring{u}^2$

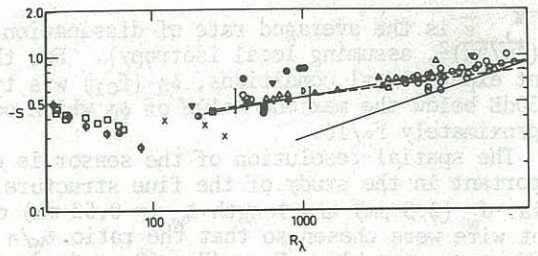

Figure 5 Variation of skewness of $\mathring{u}$ with R_λ. Circular jet: ♀, d = 2.54 cm; ⊖, 18 cm. Plane jet: ⧋. For other symbols see Van Atta & Antonia (1980).

plane jet may be sensitive to the initial conditions. There are insufficient data to suggest a definite variation of A with R_λ. For both the plane jet ($530 < R_\lambda < 730$) and the 18 cm circular jet (R_λ = 966), A is equal to about +0.35. Gibson & Masiello (1972) obtained a value for A of -1.2 in the atmospheric surface layer above the ocean surface (L was taken as the height above the surface).

Another estimate of μ can be obtained from the inertial subrange of $\phi_{\mathring{u}n}$ using Novikov's (1965) result

$$\phi_{\mathring{u}n}(k_1) \sim k_1^{-1+(n-1)\mu} \quad \text{for } n = 2,3,4 \qquad (3)$$

which for n = 2 reduces to Yaglom's (1966) expression. In the inertial subrange region, the slope of the line of best fit to $\phi_{\mathring{u}^2}$ (Fig. 4) indicates a value of μ of about 0.54 for both circular and plane jets while $\phi_{\mathring{u}^4}$ yields $\mu \simeq 0.3$. This variation of μ with n is in qualitative agreement with that inferred from Frenkiel & Klebanoff's plot. Gagne & Hopfinger (1979) measured the correlation of the moments of order p of the dissipation rate ε^p (p = 1, 1.5 and 2) and found the slopes to be different from that predicted by either the lognormal hypothesis or Novikov's result. Friehe et al (1971) obtained spectra of $(\partial u/\partial t)^n$, (n = 2, 3, 4) (they used $f_c = 0.75\, f_\eta$) in an axisymmetric jet and also found μ to decrease with increasing n.

Van Atta & Antonia (1980) examined the influence of fluctuations in the rate of local energy dissipation on higher-order structure functions of u for small values of r and on $\overline{\mathring{u}^n}$. The explicit dependence on r required by the methods of Wyngaard & Tennekes (1970), Frenkiel & Klebanoff (1975); (note that setting $r = \eta$ undermines the validity of (1)) and others was eliminated in their analysis. The predicted variation of skewness and flatness factors with R_λ did however depend, rather critically, on μ. Our experimental data for S (skewness) and F are compared in Figs. 5, 6 with the results for many different flows plotted by Van Atta & Antonia (1980). Their suggested lines of best fit ($S \sim R_\lambda^{0.15}$; $F \sim R_\lambda^{0.41}$) to the data ($R_\lambda > 100$) appear to adequately represent the present jet data (most of the data collected by Van Atta & Antonia were obtained with $f_c = f_\eta$). The value of μ corresponding to the lines of best fit in Figs. 5, 6 is 0.25, significantly lower than the values obtained from $\phi_{\mathring{u}^2}$ or σ^2 but in reasonable agreement with the value inferred from Fig. 2. Van Atta & Antonia have already indicated that μ = 0.25 may not be suitable for predicting higher order moments of $\mathring{u}$. The qualitative decrease of μ with n, indicated by the present and other data, should be reflected in the predicted variation of $\overline{\mathring{u}^6}$ or $\overline{\mathring{u}^8}$ as a function of R_λ. Reliable values of $\overline{\mathring{u}^6}$ and $\overline{\mathring{u}^8}$ at large atmospheric values of R_λ must however be obtained before this expectation is established

Fig. 7 shows the Reynolds number dependence of the fourth moment of the Kolmogorov normalised spectral density. The plane jet and circular jet (d = 18 cm) data are consistent with an increased spectral den-

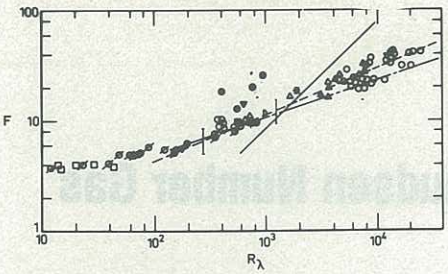

Figure 6 Variation of flatness factor of $\dot{u}$ with R_λ. Symbols are as in Figure 5.

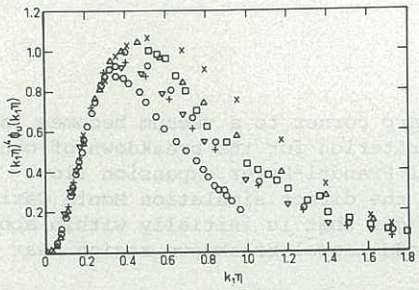

Figure 7 Fourth moment of Kolmogorov normalised spectra; ordinate × 10^2. Circular jet (d = 18 cm): x, x/d = 50; Plane jet: +, 60; ∇, 80; ⊛, 100; Δ, 160; □, circular jet, Champagne (1978); ◇, cylinder wake, Champagne (1978)

sity with R_λ as $k_1\eta$ increases. Champagne's (1978) circular jet and cylinder wake data are shown for comparison. For locally isotropic turbulence, the turbulent vorticity budget (e.g. Wyngaard & Tennekes, 1970) reduces to

$$S = -116 \int_0^\infty (\eta k_1)^4 \phi_u(\eta k_1)\, d(\eta k_1) \qquad (4)$$

Values of the left and right sides of (4) have been calculated for the plane jet and circular jet (d = 18 cm). In all cases the magnitude of left side is smaller by about 60-100% than that of right side. It should be noted that no corrections (for the effect of turbulence intensity on Taylor's hypothesis) have been made to the spectra in Fig. 7. This is because of the inadequacy in the assumptions made in obtaining the correction for spectra (Antonia et al, 1980). It is of interest to note that the analogous expression to (4) when considering temperature fluctuations is

$$\overline{(\partial u/\partial x)\,(\partial\theta/\partial x)^2} \sim \int_0^\infty k^4 F_\theta(k)\, dk \qquad (5)$$

This is essentially a simplified statement for the equation for $(\partial\theta/\partial x)^2$ in isotropic turbulence. $F_\theta(k)$ is the 3-D temperature spectrum and k is the magnitude of the wave number vector $\underline{k}$. Since the strain rate-temperature dissipation correlation on the left side of (5) increases with R_λ (Antonia & Chambers, 1979), it is reasonable to expect the high frequency behaviour of $\phi_\theta(k_1)$ as a function of R_λ to reflect that of $\phi_u(k_1)$.

4 ACKNOWLEDGEMENTS

The support of the Australian Research Grants Committee is gratefully acknowledged. The authors are grateful to Professor A.K.M.F. Hussain for providing the experimental facilities.

5 REFERENCES

ANTONIA, R. A. and CHAMBERS, A. J. (1979). On the correlation between turbulent velocity and temperature derivatives in the atmospheric surface layer. Boundary Layer Meteorology (to appear)

ANTONIA, R. A. and DANH, H. Q. (1979). Structure of temperature fluctuations in a turbulent boundary layer. Phys. Fluids Vol. 22, p.2434

ANTONIA, R. A., PHAN-THIEN, N. and CHAMBERS, A. J. (1980). Taylor's hypothesis and the probability density functions of temporal velocity and temperature derivatives in a turbulent flow. J. Fluid Mech. (to appear)

CHAMPAGNE, F. H. (1978). The fine-scale structure of the turbulent velocity field. J. Fluid Mech. Vol. 86, p.67

FRENKIEL, F. N. and KLEBANOFF, P. S. (1975). On the lognormality of the small-scale structure of turbulence. Boundary Layer Meteorology Vol. 8, p.173

FRENKIEL, F. M., KLEBANOFF, P. S. and HUANG, T. T. (1979). Grid turbulence in air and water. Phys. Fluids Vol. 22, p.1606

FRIEHE, C. A., VAN ATTA, C. W. and GIBSON, C. H. (1971). Jet turbulence: dissipation rate measurements and correlations. Proc. A.G.A.R.D., Spec. Meeting on Turbulent Shear Flow, 1971, London

GAGNE, Y. and HOPFINGER, E. J. (1979). High order dissipation correlations and structure functions in an axisymmetric jet and a plane channel flow. Proc. 2nd Int. Turbulent Shear Flow Conf., Imperial College, London, p.11.7

GIBSON, C. G. and MASIELLO, P. J. (1972). In Statistical Models and Turbulence, eds. M. Rosenblatt and C. W. Van Atta (Berlin, Springer-Verlag, 1972) p.427

GUTMARK, E. and WYGNANSKI, I. (1976). The planar turbulent jet. J. Fluid Mech. Vol. 73, p.465

HUSAIN, Z. D. and HUSSAIN, A.K.M.F. (1979). Axisymmetric mixing layer: influence of the initial and boundary conditions. A.I.A.A. Journal Vol. 17, p.48

HUSSAIN, A.K.M.F. and CLARK, A. R. (1977). Upstream influence on the near field of a plane turbulent jet. Phys. Fluids Vol. 20, p.1416

HUSSAIN, A.K.M.F. and ZEDAN, M. F. (1978). Effects of initial condition on the axisymmetric free shear layer: effects of initial momentum thickness. Phys. Fluids Vol. 21, p.1100

KOLMOGOROV, A.N. (1962). A refinement of previous hypothesis concerning the local structure of turbulence in a viscous incompressible fluid at high Reynolds number. J. Fluid Mech. Vol. 13, p.82

KUO, A. Y. and CORRSIN. S. (1971). Experiments on internal intermittency and fine-structure distribution functions in fully turbulent fluid. J. Fluid Mech. Vol. 50, p.285

NOVIKOV, E. A. (1965). High-order correlations in turbulent flow. Izv. Atmos. Ocean Phys. Ser. Vol. 1, p.788

OBUKHOV, A. M. (1962). Some specific features of atmospheric turbulence. J. Fluid Mech. Vol. 13, p.77

TENNEKES, H. and LUMLEY, J. L. (1972). A First Course in Turbulence, M.I.T. Press

VAN ATTA, C. W. and ANTONIA, R. A. (1980). Reynolds number dependence of skewness and flatness factors of turbulent velocity derivatives. Phys. Fluids, Vol. 23, p.252

WYNGAARD, J. (1968). Measurements of small-scale turbulence structure with hot wires. J. Sci. Instrum. Vol. 1, p.1105

WYNGAARD, J. and TENNEKES, H. (1970). Measurement of small-scale structure of turbulence at moderate Reynolds numbers. Phys. Fluids, Vol. 13, p.1962

YAGLOM, A. M. (1966). The influence of fluctuations in energy dissipation on the shape and turbulence characteristics in the inertial interval. Sov. Phys. Dokl. Vol. 11, p.26